P and T waves annotation and detection in MIT-BIH arrhythmia database

Mohamed Elgendi

Department of Computing Science, University of Alberta, Canada

E-mail: moe.elgendi@gmail.com

Abstract

A robust and numerically-efficient method based on two moving average filters followed by a dynamic event duration threshold has been developed to detect P and T waves in ECG signals. Detection of P and T waves is affected by the quality of the ECG recordings and the abnormalities in the ECG signals. The proposed method detects P and T waves in Arrhythmia ECG Signals that suffer from: 1) non-stationary effects, 2) low signal-to-noise ratio, 3) premature atrial complexes 4) premature ventricular complexes, 5) left bundle blocks, and 6) right bundle blocks. Interestingly, the P and T waves detector obtained a a sensitivity of 98.05 per cent and a positive predictivity of 97.11 per cent for P waves and a sensitivity of 99.86 per cent and a positive predictivity of 99.65 per cent for T waves over 10 records of MIT-BIH arrhythmia database with 21,702 beats. The P and T detection algorithm performed very well compared to traditional detection algorithms.

Keywords: electrocardiogram, P detection, T detection, ECG analysis, P wave annotation, T wave annotation, arrhythmia

1. Introduction

According to the World Health Organization, cardiovascular diseases (CVD) are the number one cause of death globally, more people die annually from CVDs than from any other cause. An estimated 17.3 million people died from CVDs in 2008, representing 30% of all global deaths. Of these deaths, an estimated 7.3 million were due to coronary heart disease and 6.2 million were due to stroke.

In Australia, CVD is the leading cause of death in Australia, and the second leading cause of disease burden [1]. Through 2007, CVD was the underlying cause of 34 per cent of all deaths in Australia (46,626 deaths [2]) and it is estimated that around 1.4 million Australians experience a disability associated with the cardiovascular system. These rates are consistent with those of other western developed countries such as New Zealand, the United States (US), the United Kingdom (UK) and the Scandinavian nations [3].

CVD is the most expensive disease group in terms of direct health-care expenditure. In 2008, it cost Australia about $5.9 billion [4]. As a consequence of the direct and indirect costs of CVD, medical researchers have placed significant importance on cardiac health research. This has produced a strong focus on preventative, medicinal and technological advances, both in Australia and abroad. One such research pathway is leading researchers towards improving the conventional cardiovascular-diagnosis technologies used in hospitals/clinics.

The most commonly performed cardiac test is ECG as it is a useful screening tool for a variety of cardiac abnormalities, simple, risk-free and inexpensive. The advances in technology have done much change to the way we collect, store and diagnose ECG signals, especially the advances in memory/storage technology have enabled us to store more ECG signals than ever before.

Scientists are collecting more information in order to understand the mechanism of the cardiovascular diseases which will ultimately lead to effective treatments. However, analysing large ECG recordings, collected over one or more days, is a time consuming process. Therefore, a robust and numerically-efficient algorithm is highly required to analyse ECG signals.

P and T waves are two of the three main waveforms in an ECG. The normal heartbeat (or cardiac cycle) consists of a P wave, a QRS complex, and a T wave. The P wave represents the wave of depolarisation that spreads from the sino-atrial node throughout the atria. The morphology of the P wave provides relevant information concerning intra-atrial conduction, hypertrophic conditions of the atria and atrio-ventricular conduction, among others [5].

The T wave corresponds to the ventricular repolarisation phase of the heart cycle. In some pathological conditions the morphology of the T wave may change from beat to beat [5]. Due to the low amplitude of P or T waves, distinguishing the morphology of P or T waves in noisy ECG signals is considered challenging.

The purpose of this work is to develop an effective P and T wave detection algorithm and test it on MIT−BIH arrhythmia ECG signals. As mentioned in Section 4.1.1, the database contains different types of arrhythmia with abnormal morphologies of P and T waves. Therefore, evaluating the P and T wave detection algorithm will reflect its robustness against arrhythmia P and T waves.

A number of algorithms are found in the literature. Most of these algorithms delineate either P or T waves of the ECG, and a few approaches delineate both P and T waves. In 1990, Trahanias and Skordalakis [6] applied a syntactic approach to ECG pattern recognition and parameter measurement for the detection of P, QRS and T waves. Their approach has been evaluated using the CSE database [7] to compare the onsets and offsets of P, QRS, and T waves obtained by their program with those provided by the referenced library. Murthy and Prasad [8] used the discrete cosine transform (DCT) for delineation of P waves and applied it to a database of 500 beats. In about 0.5 per cent of the beats, the algorithm failed to model the P wave, usually when its amplitude was very small. Their method was applied to a few ECG segments from the MIT−BIH database and to their own data, consisting of 500 beats. Thakor and Zhu [9] used adaptive filters for delineation of P waves. They used their own data.

Li et al. Proposed a method for detecting monophasic P and T waves based on quadratic spline wavelets with compact support and one vanishing moment was proposed by [10]. They did not mention whether they tested the algorithm on any ECG database. Carlson et al. [11] used a classification method for P wave morphology based on the impulse response analysis of the P wave and linear discrimination. They reported a sensitivity of 95 per cent, and a specificity of 90 per cent after using 37 records out of 40 from their own collected data. De Azevedo et al. [12] used a neural network with asymmetric basis functions to extract the features of the P waves. They tested the algorithm on the MIT−BIH database but did not mention the detection rate. Vila et al. [13] proposed an algorithm for the detection and characterisation of the T waves based on mathematical modelling. Their approach has been evaluated using the PhysioNet QT database.

Strumillo proposed a nonlinear signal decomposition method based on nested median filters for detecting the T wave offset in ECG signals [14]. Their approach has been evaluated using the PhysioNet QT Database without mentioning the detection rate. Martinez et al. presented a generalized method for the delineation of P and T waves based on quadratic spline wavelets and the derivative of a Gaussian as a smoothing function [15]. They reported a sensitivity of 98.87 per cent for the P waves

and a sensitivity of 99.77 per cent for the T waves using the PhysioNet QT database. The Biorthogonal WT was applied by Sovilj et al. to detect P waves. They reported a sensitivity of 98.5 per cent without mentioning the source of their data [16]. The first derivative with adaptive quantised thresholds was used by Chouhan et al. [17], who reported a P wave detection rate of 96.95 per cent with false positive and false negative percentages of 2.62 per cent and 3.01 per cent respectively. Similarly, a T wave detection rate of 98.01 per cent with false positive and false negative percentages of 3.08 per cent and 1.93 per cent was reported after using 125 files from the CSE Database [7]. They did not apply their algorithm to the MIT−BIH Arrhythmia Database.

The detection of P and T waves has been investigated in the past two decades. Many attempts have been made to find a satisfying universal solution for P and T waves' detection. Difficulties arise mainly because of the diversity of the P and T waveforms, abnormalities, low SNR and the artifacts accompanying the ECG signals. Moreover, producing P and T waves detection performance with high rates after excluding some segments or beats from the used records.

The performance of the existing P and T wave detection algorithms is still inefficient and needs to be tested on long recordings rather than short ECG segments, such the well-known MIT-BIH database. Therefore, the main focus of this study is to develop a robust and numerically-efficient algorithm tested over MIT-BIH arrhythmia database after being annotated. Moreover, compare the developed algorithm against the existing P and T detection methods.

This paper is structured as follows. The next section discusses the ECG database and the annotation of P and T waves. Section 3 demonstrates the different types of noise in ECG, while Section 4 elaborates on the new methodology of detecting P and T waves. Section 5 elaborates on the results and discussion respectively. Finally discussion and conclusion covered in Section 6.

2. Data

Several standard ECG databases are available for the evaluation of QRS detection algorithms for ECG signals. Most of these databases contain annotated files for R peaks but not for P and T waves. The MIT−BIH Arrhythmia Database [18] will be used in this study for the following reasons:

- The MIT−BIH Database contains 30-minute recordings for each patient which is considerably longer than the records in many other databases, such as the Common Standards for Electrocardiography (CSE) database, which contains 10-second recordings [7].
- The MIT−BIH Arrhythmia Database contains records of normal ECG signals and records of ECG signals that are affected by non-stationary effects, low signal-to-noise ratio (SNR), premature atrial complexes, premature ventricular complexes, left bundle blocks, and right bundle blocks. This provides an opportunity to test the robustness of QRS, P and T wave detection methods.
- The database contains 23 records (the '100 series') that were chosen at random from a set of more than 4,000 24-hour Holter tapes, and 25 records (the '200 series') that were selected from the same set, including a variety of rare and clinically important ECG segments [19]. Several records in the 200 series have abnormal rhythms and QRS morphologies, and they suffer from a low SNR. These issues are expected to present significant difficulties for any ECG signal analysis algorithms [19]. Table 1 provides an overview of the different beat types in the MIT−BIH database.

Table 1 ECG database. A statistical overview of different beat types in the MIT−BIH Arrhythmia Database [18].

Record	Normal beat	LBBB	RBBB	Atrial premature beat	Abberated atrial premature beat	Nodal premature beat	Supraventricular premature beat	Ventricular premature beat	Fusion of ventricular or normal beat	Ventricular flutter wave	Atrial escape beat	Nodal escape beat	Ventricular escape beat	Paced rhythm	Fusion of paced or normal beat	Pause	Unclassified beat
100	2239	-	-	33	-	-	-	1	-	-	-	-	-	-	-	-	-
101	1860	-	-	3	-	-	-	-	-	-	-	-	-	-	-	-	2
102	99	-	-	-	-	-	-	4	-	-	-	-	-	2028	56	-	-
103	2082	-	-	2	-	-	-	-	-	-	-	-	-	-	-	-	-
104	163	-	-	-	-	-	-	2	-	-	-	-	-	1380	666	-	18
105	2526	-	-	-	-	-	-	41	-	-	-	-	-	-	-	-	5
106	1507	-	-	-	-	-	-	520	-	-	-	-	-	-	-	-	-
107	-	-	-	-	-	-	-	59	-	-	-	-	-	2078	-	-	-
108	1739	-	-	4	-	-	-	17	2	-	-	1	-	-	-	11	-
109	-	2492	-	-	-	-	-	38	2	-	-	-	-	-	-	-	-
111	-	2123	-	-	-	-	-	1	-	-	-	-	-	-	-	-	-
112	2537	-	-	2	-	-	-	-	-	-	-	-	-	-	-	-	-
113	1789	-	-	-	6	-	-	-	-	-	-	-	-	-	-	-	-
114	1820	-	-	10	-	2	-	43	4	-	-	-	-	-	-	-	-
115	1953	-	-	-	-	-	-	-	-	-	-	-	-	-	-	-	-
116	2302	-	-	1	-	-	-	109	-	-	-	-	-	-	-	-	-
117	1534	-	-	1	-	-	-	-	-	-	-	-	-	-	-	-	-
118	-	-	2166	96	-	-	-	16	-	-	-	-	-	-	-	10	-
119	1543	-	-	-	-	-	-	444	-	-	-	-	-	-	-	-	-
121	1861	-	-	1	-	-	-	1	-	-	-	-	-	-	-	-	-
122	2476	-	-	-	-	-	-	-	-	-	-	-	-	-	-	-	-
123	1515	-	-	-	-	-	-	3	-	-	-	-	-	-	-	-	-
124	-	-	1531	2	-	29	-	47	5	-	-	5	-	-	-	-	-
200	1743	-	-	30	-	-	-	826	2	-	-	-	-	-	-	-	-
201	1625	-	-	30	97	1	-	198	2	-	-	10	-	-	-	37	-
202	2061	-	-	36	19	-	-	19	1	-	-	-	-	-	-	-	-
203	2529	-	-	-	2	-	-	444	1	-	-	-	-	-	-	-	4
205	2571	-	-	3	-	-	-	71	11	-	-	-	-	-	-	-	-
207	-	1457	86	107	-	-	-	105	-	472	-	-	105	-	-	-	-
208	1586	-	-	-	-	-	2	992	373	-	-	-	-	-	-	-	2
209	2621	-	-	383	-	-	-	1	-	-	-	-	-	-	-	-	-
210	2423	-	-	-	22	-	-	194	10	-	-	-	1	-	-	-	-
212	923	-	1825	-	-	-	-	-	-	-	-	-	-	-	-	-	-
213	2641	-	-	25	3	-	-	220	362	-	-	-	-	-	-	-	-
214	-	2003	-	-	-	-	-	256	1	-	-	-	-	-	-	-	2
215	3195	-	-	3	-	-	-	164	1	-	-	-	-	-	-	-	-
217	244	-	-	-	-	-	-	162	-	-	-	-	-	1542	260	-	-
219	2082	-	-	7	-	-	-	64	1	-	-	-	-	-	-	133	-
220	1954	-	-	94	-	-	-	-	-	-	-	-	-	-	-	-	-
221	2031	-	-	-	-	-	-	396	-	-	-	-	-	-	-	-	-
222	2062	-	-	208	-	1	-	-	-	-	-	212	-	-	-	-	-
223	2029	-	-	72	1	-	-	473	14	-	16	-	-	-	-	-	-
228	1688	-	-	3	-	-	-	362	-	-	-	-	-	-	-	-	-
230	2255	-	-	-	-	-	-	1	-	-	-	-	-	-	-	-	-
231	314	-	1254	1	-	-	-	2	-	-	-	-	-	-	-	2	-
232	-	-	397	1382	-	-	-	-	-	-	-	1	-	-	-	-	-
233	2230	-	-	7	-	-	-	831	11	-	-	-	-	-	-	-	-
234	2700	-	-	-	-	50	-	3	-	-	-	-	-	-	-	-	-

Figure 1 Annotation of P and T waves in normal beats. Determining the normality of the beats is based on the annotation provided by the MIT-BIH database and described in Table 1. '+' represents the P wave and '*' represents the T wave.
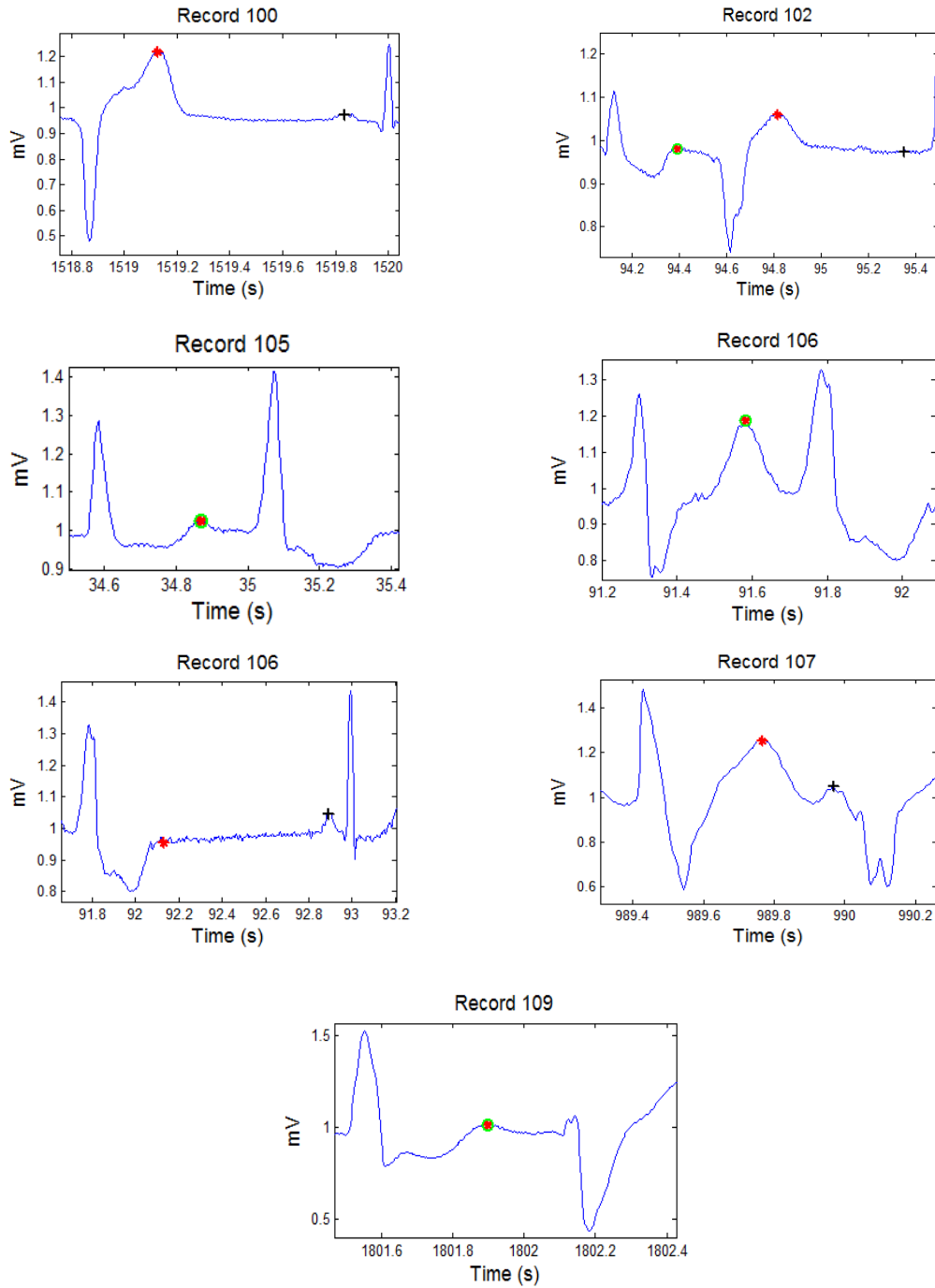
Figure 2 Annotation of P and T waves in PVC beats. Determining the abnormality of the beats is based on the annotation provided by the MIT-BIH database and described in Table 1. '+' represents the P wave and '*' represents the T wave, while the circle with asterisk represents merged P and T waves.
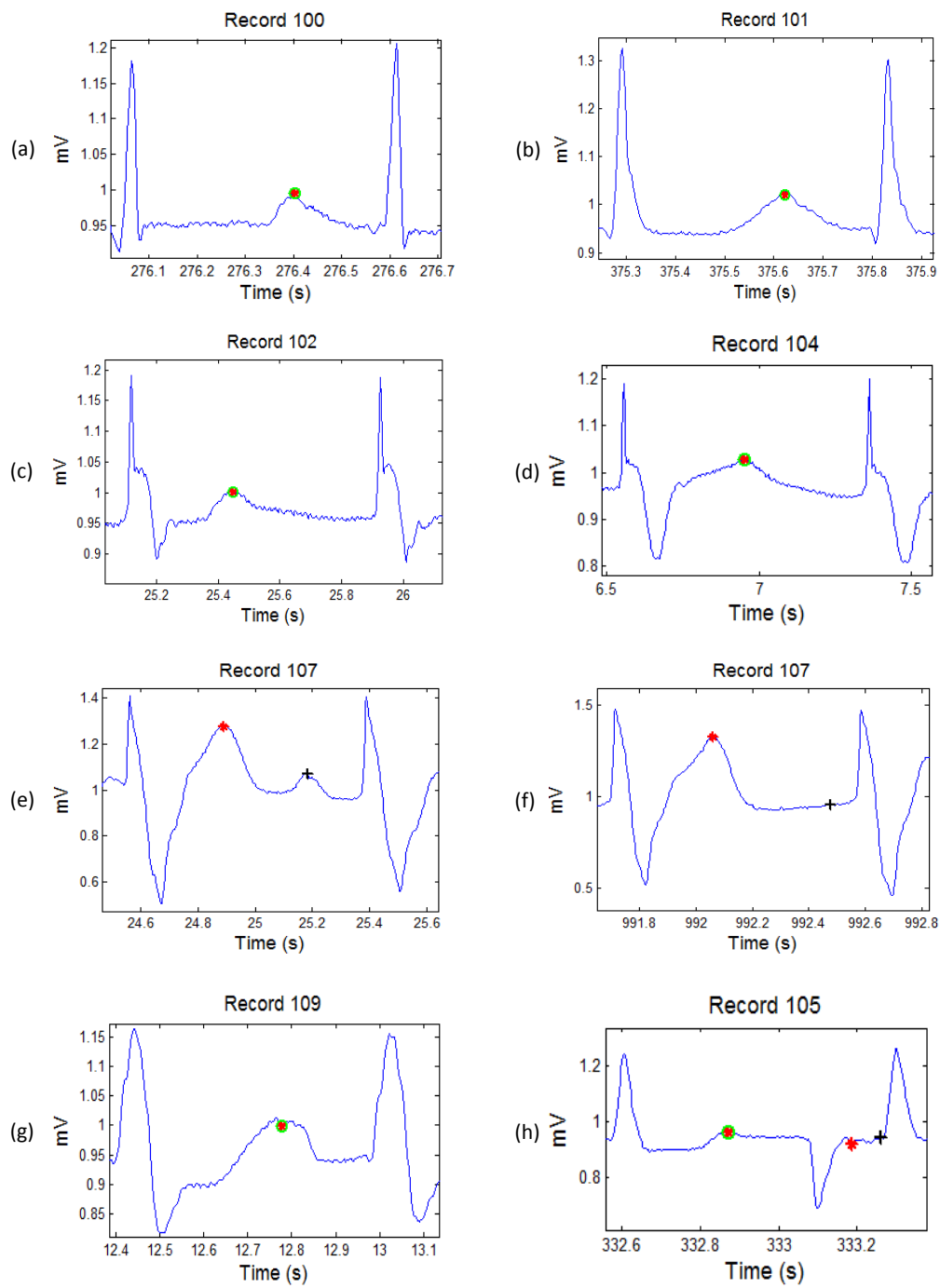
Figure 3 Annotation of P and T waves in different types of beats. Determining the abnormality of the beats is based on the annotation provided by the MIT-BIH database and described in Table 1. (a-b) atrial premature beats, (c-f) paced beat, (g) left bundle branch block beat, (h) isolated-like QRS beat .'+' represents the P wave and '*' represents the T wave, while the circle with asterisk represents merged P and T waves.
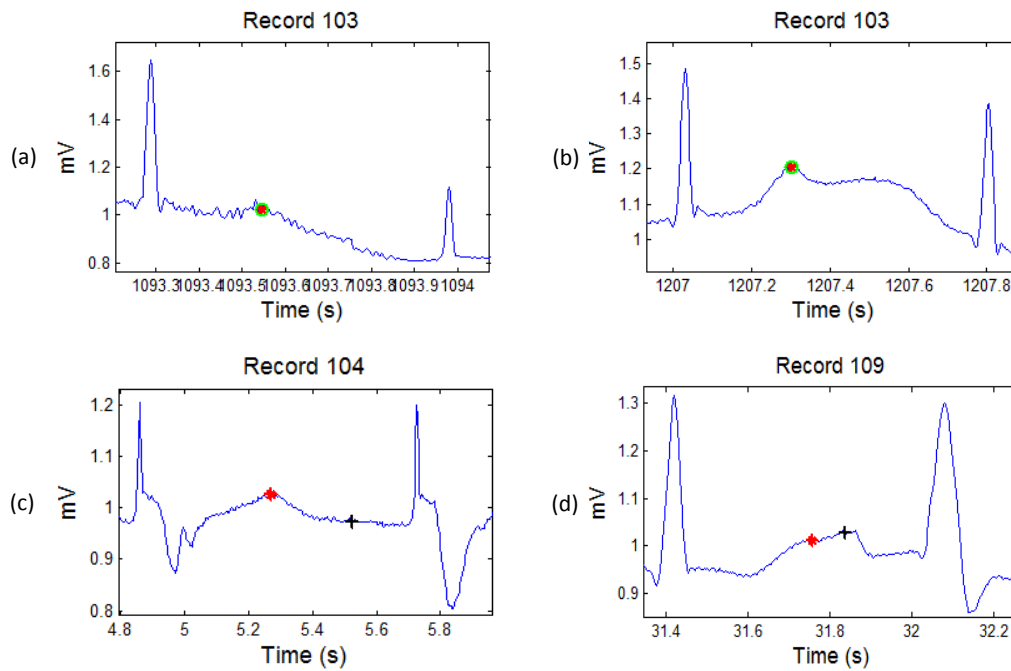
Figure 4 Annotation of P and T waves in controversial beats. Determining the controversial beats is based on the annotation provided by the MIT-BIH database and described in Table 1. (a-b) normal beats where P wave is not salient, (c) Fusion of paced and normal beat, (d) Fusion of ventricular and normal beat.'+' represents the P wave and '*' represents the T wave, while the circle with asterisk represents merged P and T waves.

The MIT−BIH Arrhythmia Database contains 48 ECG recordings with total of 110,007 beats. These 30-minute recordings were sampled at 360 Hz with an 11-bit rate resolution over a 10 mV range. Lead I from each record is used here because the quality of the ECG signals was higher in Lead I compared to Lead II. No episodes (measurements) were excluded.

The MIT−BIH Arrhythmia Database is annotated. R peaks are fully annotated; therefore, the QRS detection algorithm has been tested automatically. Unfortunately, the P and T waves are not annotated; thus, two independent annotators annotated the P and T waves in 10 records of MIT-BIH arrhythmia database, specifically records 100 to 109. The symbols used for annotation are as follows:

     a.   '+' shows the detected P waves

     b.   '*' shows the detected T waves

     c.   circle with asterisk shows the detected P and T waves

Annotation is a difficult task due to inter-annotator discrepancy, as the two annotators will never agree completely on what and how to annotate the P and T waves in each record. Figures 1, 2, 3, 4 show how the annotated P and T waves after the discrepancies were adjudicated.
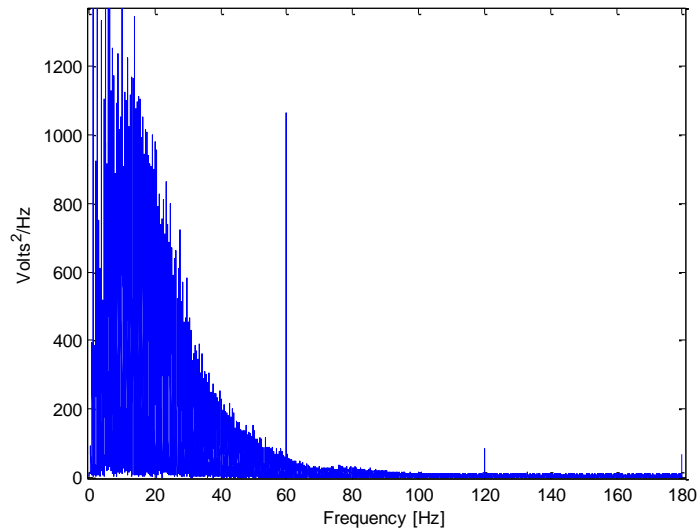
Figure 5 Power spectrum of the ECG signal. The spectrum illustrates peaks at the fundamental frequency of 60 Hz as well as the second and third harmonics at 120 Hz and 180 Hz, respectively.

3. Sources of Noise in ECG

ECG signals can be contaminated with several types of noise which may affect the accuracy of the main events detection and overall diagnosis. The noise could be physiological, caused by the instrumentation used or the experiment's environment of. Removing the various types of noise that corrupt the ECG without degrading the signal of interest is challenging. The main sources of noise, which are relevant for the detection of P and T waves are discussed below.

3.1 Powerline Interference

Powerline interference noise is caused by interference from mains power sources being induced onto the recording leads of the ECG which introduces a sinusoidal component into the recording. The ECG database used for this research was collected in the United States (US). Therefore, ECG signals used for this thesis have a frequency component of 60 Hz. The periodic interference is clearly displayed as a spike in Figure 5, not only at its fundamental frequency of 60 Hz, but also on its harmonics (e.g. 120 Hz, 180 Hz). Its amplitude can be up to 50 percent of the peak-to-peak ECG amplitude [20].

3.2 Physiological Interference

The human body is a complex accumulation of systems and processes. Several physiological processes could be active at a given moment, each one producing many signals of different types [21]. The appearance of signals from systems or processes other than those related to the heart may be termed as physiological interference, as discussed below.

3.2.1 Muscle Noise

Muscles other than the heart produce electrical impulses in the body; these impulses can also be detected by the ECG leads. Unlike cardiac muscles, other muscles do not have a regulated cycle; therefore, the generated impulses will not be represented as characteristic waveforms. The noise is usually of a low amplitude and high frequency, and it can be sporadic or consistent throughout the recording as shown in Figure 6.
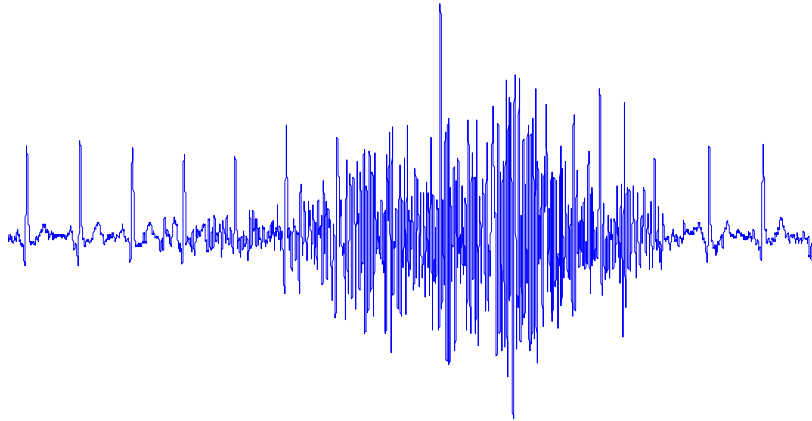
Figure 6 Muscle noise. Coughing, tensing of muscles and movement of limbs cause the corresponding electromyogram (EMG) signal to appear as undesired noise.

3.2.2   Motion Artifact

Low-frequency artifacts and baseline drift may be caused by poor contact of the chest leads. A small arm or leg movement may cause a simple baseline wander as shown in Figure 7. Variations in temperature can occasionally cause baseline drift. In general, baseline wander makes it difficult to detect P, QRS and T waves. To remove the baseline wandering, a low pass filter can be implemented.

Contact between the skin and the electrode is important to obtain an ECG signal of good quality. The loss of contact can be permanent, or can be intermittent, as would be the case when a loose electrode is brought in and out of contact with the skin as a result of movements and vibration. Large movement can cause a rapid baseline transition (step) which decays exponentially to the baseline value, as shown in Figure 8. Chang Yong *et al.* [22] proposed to use conductive yarn rubber electrodes to reduce the motion artifact. Moreover, loss of contact associated with movement may generate isolated QRS-like artifacts as shown in Figure 9.
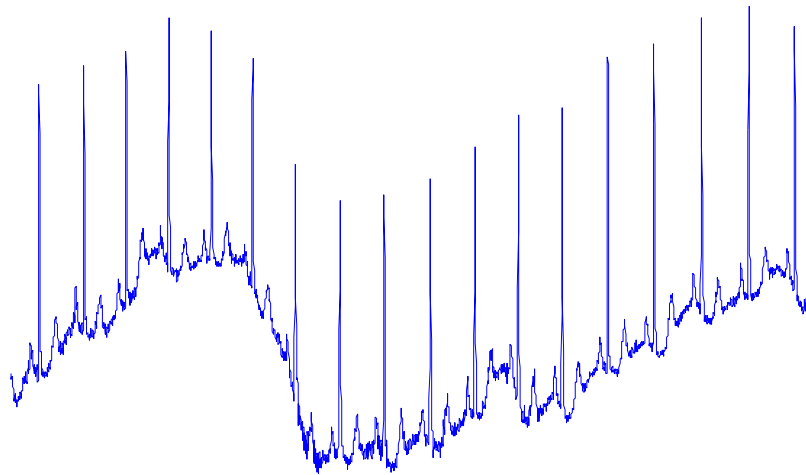
Figure 7 Baseline wandering. The usual cause of motion artifacts is assumed to be vibrations or movement of the subject. The shape of the baseline disturbance caused by motion artifacts is assumed to be a biphasic signal resembling one cycle of a sine wave.
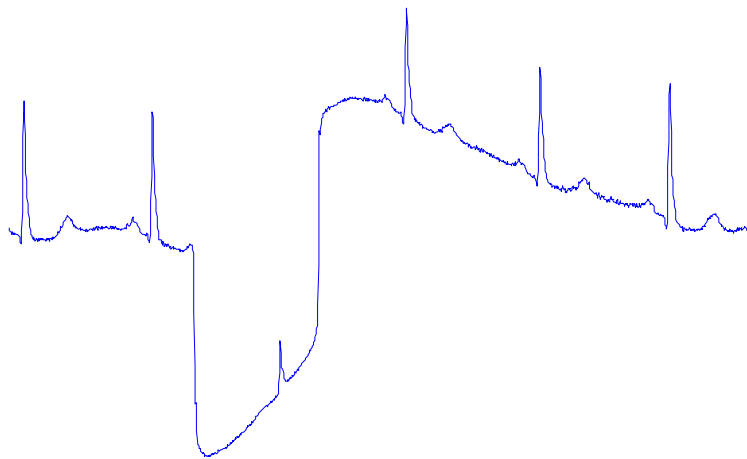
Figure 8 Large movement of the chest. The low frequency noise is generated by bad contact between skin and electrode.
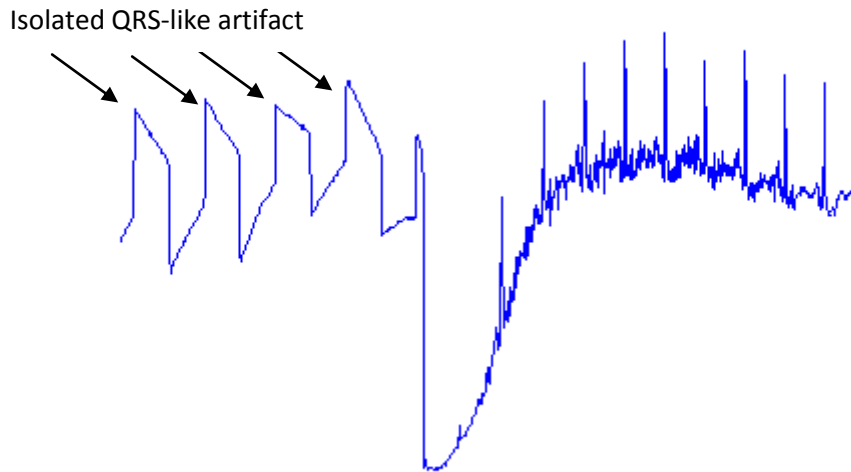
Figure 9 Large movement with isolated QRS-like artifacts. This segment starts with isolated QRS-like artifacts followed by low frequency followed by high frequency

4. Methodology

In economics, moving average is a common analysis tool used by traders to identify trend directions. More than one moving average can be used to generate buy and sell signs [23]. Two moving averages have been used together to generate crossover signs [24,25]. These crossovers are the buy and sell indicators. A crossover occurs when a faster (shorter) moving average crosses a slower (longer) moving average [26].

The use of two moving averages succeeds in detecting the critical events in trading. Moreover, in ECG signal analysis, two moving averages have been used as a bandpass filter to extract the QRS features in [27,28]. In addition, the implementation of the moving average can be highly numerically efficient (simple, fast and fewer calculations required). Therefore, the idea of using two moving averages is promising.

In this section, a new, numerically-efficient and robust algorithm is proposed to detect QRS complexes in ECG signals based on two moving-average filters. The first moving average is used to extract the QRS features while the second moving average works as a threshold to the first one. This creates blocks of interests followed by a QRS complex duration threshold to detect QRS complexes.

The introduced algorithm is a generic algorithm based on the characteristics of the ECG features; that is, the average duration of the QRS complex and heart beat in healthy subjects. The thresholds used in this algorithm are adaptive signal-dependent. The ECG signal passes successively through a sequence of processing steps, including bandpass filtering, differentiating, squaring, generating blocks of interest and applying dynamic thresholding, to distinguish the QRS complexes, as shown in Figure 10. The maximum absolute values within the considered QRS blocks are considered R peaks
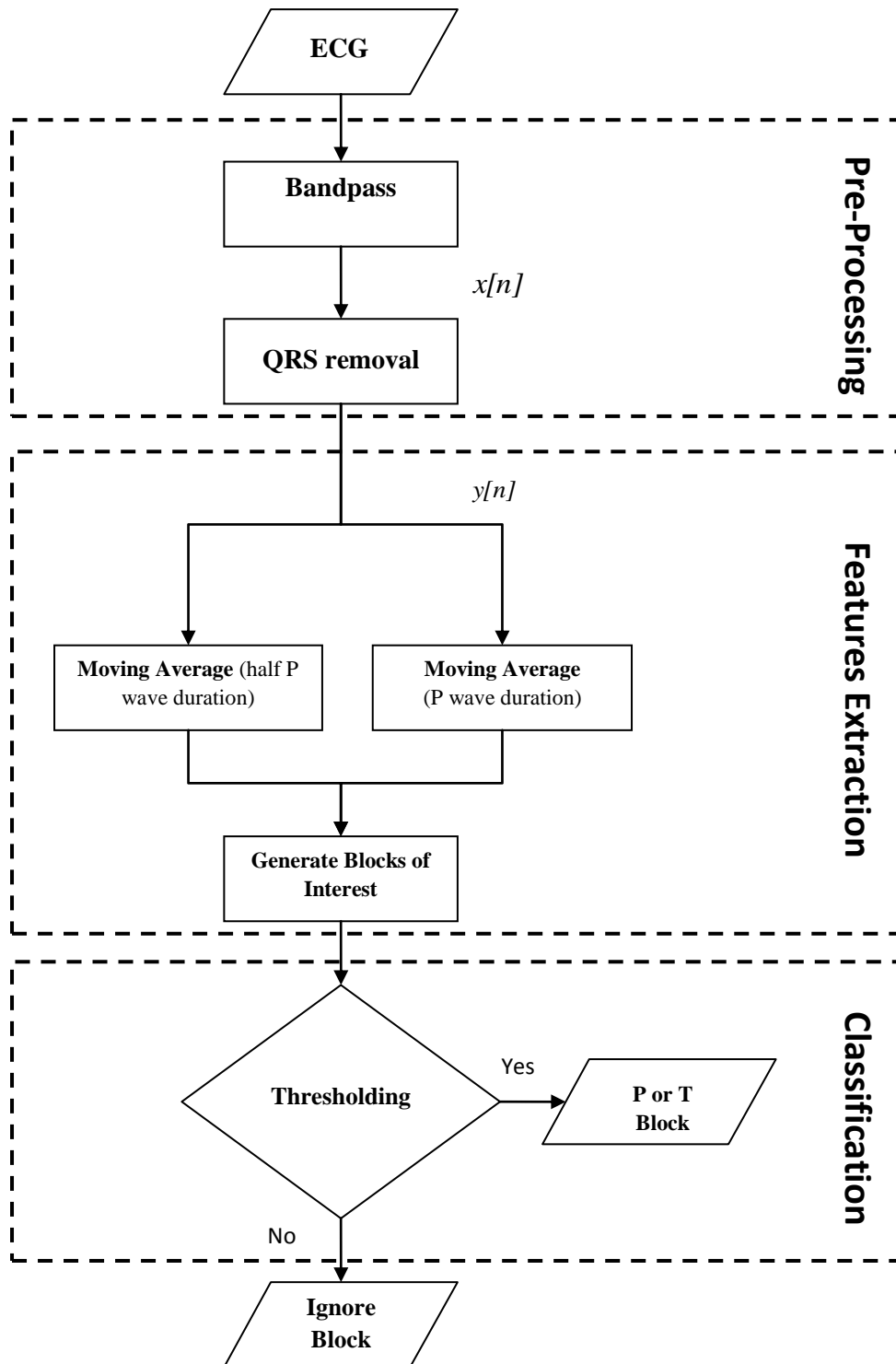
Figure 10 Flowchart for new P and T waves detection algorithm. This P and T detection algorithm is a time-domain algorithm that consists of three main stages: pre-processing, feature extraction and classification.

Bandpass Filter

As discussed, a recommended bandpass filter is typically a bidirectional Butterworth implementation. These filters offer good transition-band characteristics at low coefficient orders, which make them efficient to implement [29].

The main frequencies of the P and the T wave lie in the range of 0.5 Hz to 10 Hz [30]. In this thesis, the baseline wander and high frequencies that do not contribute to P and T wave detection are removed using a second-order Butterworth filter with passband 0.5−10 Hz.

$ECG[n]$ → Butterworth Filter → $s[n]$ → Time reversal → Butterworth Filter → $x[n]$
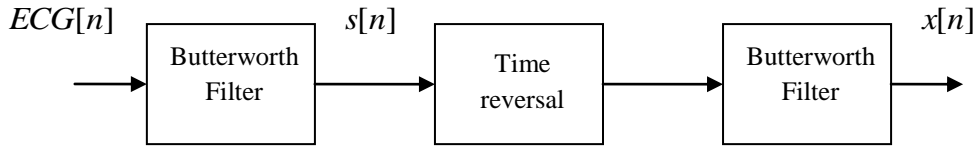
Figure 11 Demonstrating the zero-phase filtering in ECG signals

The phase lag effect of the Butterworth filter can be cancelled by following the process shown in Figure 11. The $x[n]$ output will be a filtered version of $ECG[n]$ with no phase distortion. The same Butterworth filter is used twice in this scheme: the time reversal step is a straight left-right flipping of the time domain sequence, as follows:

$$s[n] = \sum_{k=0}^{N} b_k \, ECG[n-k] - \sum_{k=1}^{N} a_k s[n-k] \qquad \text{Eq. 1}$$

$$x[n] = \sum_{k=0}^{N} b_k \, s[n-k] - \sum_{k=1}^{N} a_k x[n-k] \qquad \text{Eq. 2}$$

QRS Removal

To make the P and T waves the dominant feature of the signal, the QRS complex is removed. Therefore, R peaks must be detected before applying the P and T waves algorithm. Fourtunately, R peaks are annotated in the MIT−BIH Arrhythmia Database.
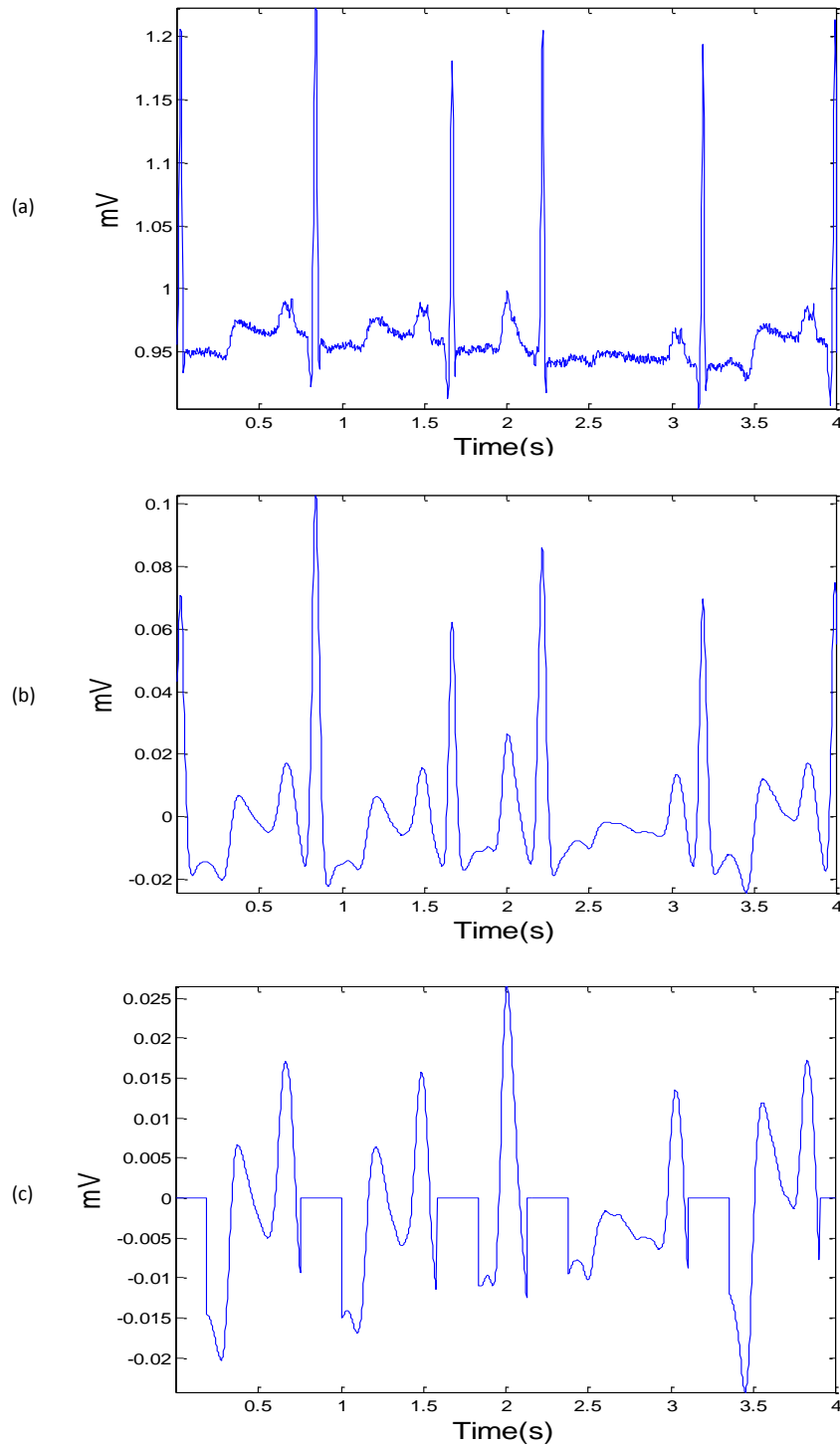
Figure 12 Pre-processing stage of the algorithm structure. (a) Original ECG signal, (b) filtered ECG signal with bidirectional Butterworth bandpass filter, (c) QRS removal.
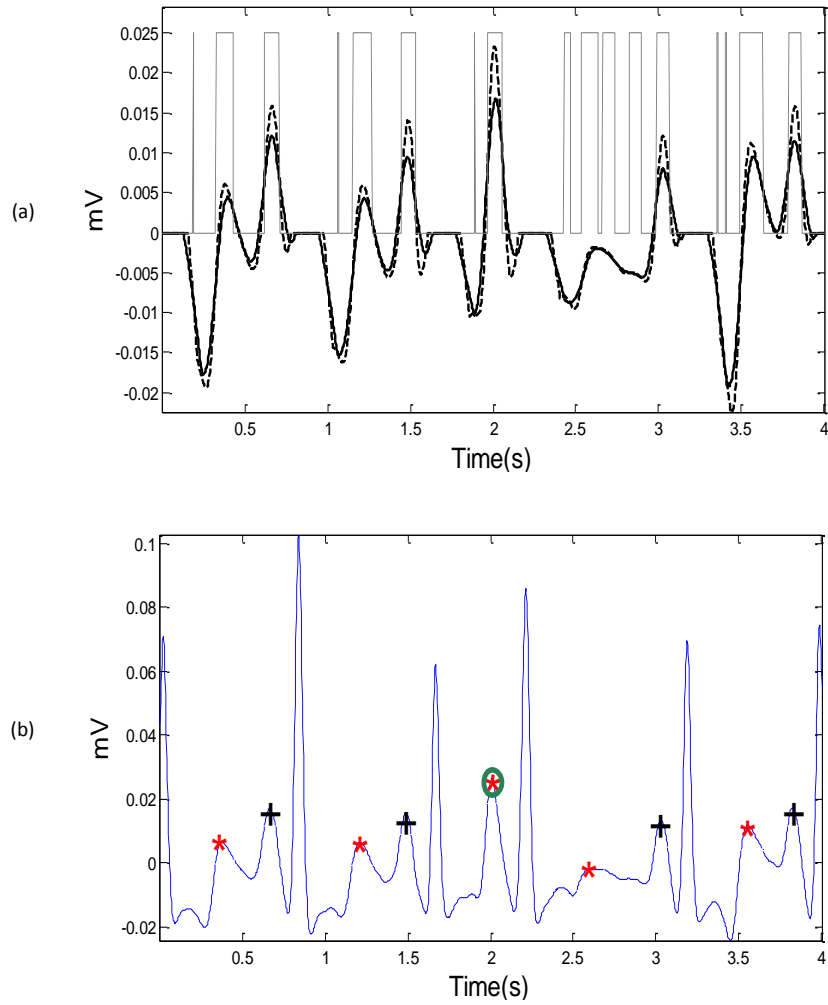
Figure 13 Features extraction and classification stages of the algorithm structure. (a) Generating blocks of interest using two moving averages, (b) the final result of the proposed algorithm to detect P and T waves. '+' represents the P wave and '*' represents the T wave, while the 'circle with asterisk' represents merged P and T waves.

Removing the QRS complex duration is performed by setting the signal to zero for the duration of the QRS complex [31]. The duration's 0.083 ms before R peak and 0.166 ms after R peak are set to zeros in all beats.

$$y[n] = QRS\ Removal(x[n])$$ Eq. 3

Figure 12 (c) shows the result of removing QRS complexes from the filtered signal of Figure 12 (b).

Select Potential Blocks

The onset and offset of the potential P and T waves in the ECG signals will be demarcated using two moving averages based on the normal duration of the ECG features. The normal limit of the P wave duration for a healthy adult is 110±20 ms at a heart rate of 60 beats per minute [32]. The normal limit of the corrected QT interval is 400±40 ms.

The average duration of the event is the suitable window size to detect the event. The average window size corresponding to the P wave duration approximately 110

ms, and the average window size corresponding to the QT_c duration is approximately 400ms. As the P and T waves will be detected simultaneously, and the expected duration of the P wave is smaller than the T wave, the window size of the two moving averages will be adjusted related to the P wave duration.

In healthy subjects (P and T waves exist in the ECG signal), the moving average that can demarcate the P wave can also demarcate the T wave.

The detection of P and T waves will depend on two moving averages. The first moving average will be used to demarcate the P and T waves, while the second moving average (with a larger window size) will be used as the threshold for the first moving average, as discussed below.

i) First moving average: The first moving-average integration is used to demarcate the P and T waves with a sharp wave, shown as the dotted line in Figure 13 (a).

$$MA_{Peak}[n] = \frac{1}{W_1}(y[n-(W_1-1)/2]+....+y[n]....+y[n+(W_1-1)/2]) \qquad \text{Eq. 4}$$

where $W_1 = 55\,ms * SF$ which is half the window width of the P interval. Its value is rounded to the nearest odd integer. A smaller window size is chosen than the expected healthy duration in order to demarcate small P and T duration in cases of severe arrhythmia.

ii) Second moving average: The purpose of the second moving average (MA_{Pwave}) is to be used as a threshold for the first moving average MA_{Peak} integration, shown as the solid line in Figure 13 (a):

$$MA_{Pwave}[n] = \frac{1}{W_2}(y[n-(W_2-1)/2]+....+y[n]....+y[n+(W_2-1)/2]) \qquad \text{Eq. 5}$$

where $W_2 = 110\,ms * SF$ is the window width of the P interval. Its value is rounded to the nearest odd integer.

As discussed above, the window size of the first moving average should be less than the average healthy duration for the P wave (which is half of the P wave duration) while the window size of the second moving average equals the average healthy P wave duration. The first moving average will demarcate the P and T waves (especially in cases of arrhythmia with smaller durations), and the second moving average then works as a threshold for the first moving average. It has been observed that when the window W_2 is less than 110ms, false negative will increase. Conversely, if the window size W_2 is greater than 110 ms, the FNs will decrease and the FPs will increase.

When the amplitude of the first moving-average filter (MA_{Peak}) is greater than the amplitude of the second moving-average filter (MA_{Pwave}), that part of the signal is selected as a block of interest, as follows:

IF $MA_{Peak}[n] > MA_{Pwave}[n]$ **THEN**

Blocks[n] =0.25

ELSE

Blocks[n] =0

END

Figure 13 (a) shows the result of applying the two moving averages.
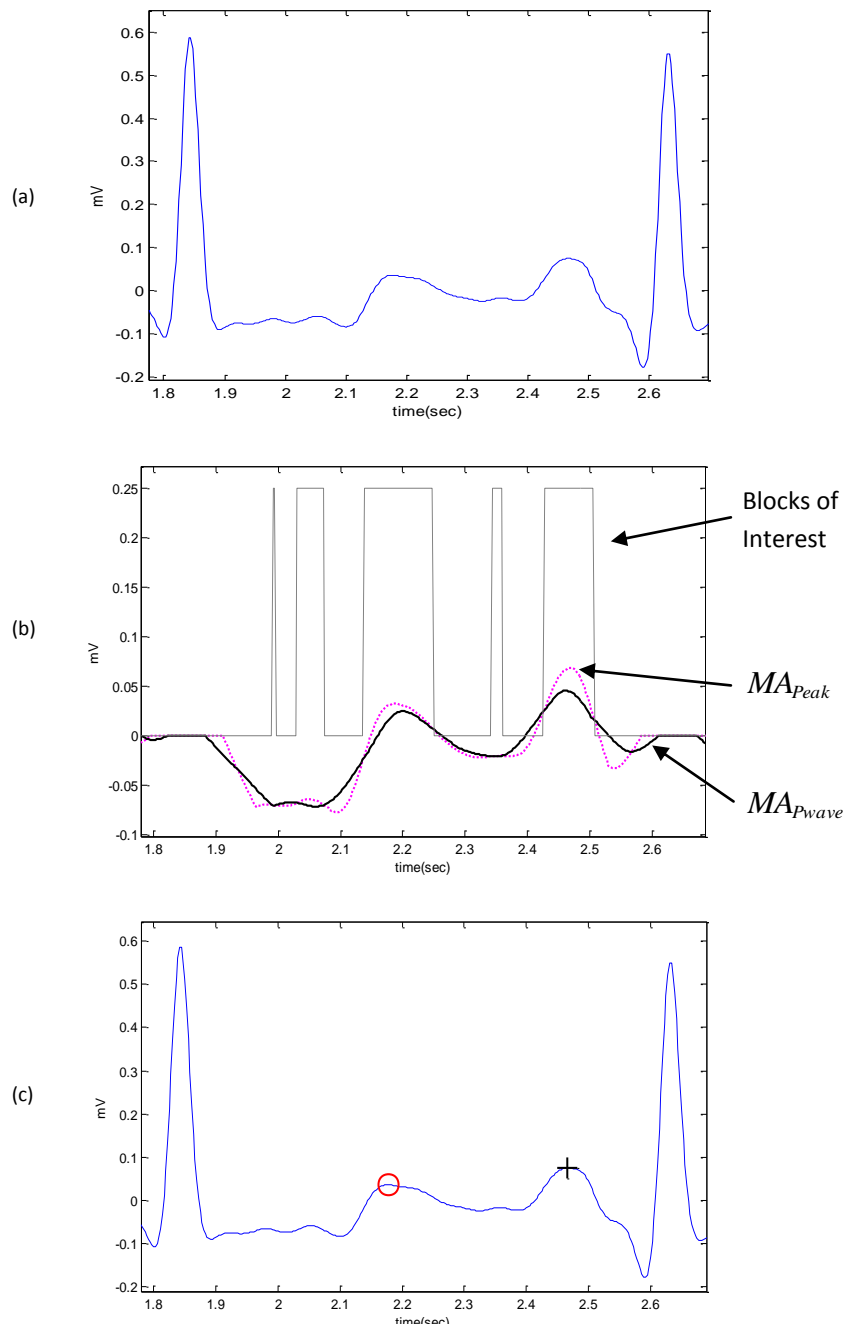
Figure 14 Demonstrating the effectiveness of using two moving averages to detect P and T waves.
(a) Filtered RR ECG signal with Butterworth bandpass filter, (b) generating blocks of interest after using two moving averages: the dotted line is the first moving average and the solid line is the second moving average, (c) the detected P and T waves after applying the thresholds.

If the interest is the sinus activity for heart rate variability, then the PP interval should be considered a better measure compared to the RR interval [33]. However, in this research, the main interest is the pump function and the blood volume; thus, QRS, and consequently the RR interval are more important. One RR interval shown in Figure 14 (b) demonstrates the idea of using two moving averages to generate blocks of interest. It can be seen that not all of the generated blocks of interest are potential P or T waves. The blocks will be considered according to their relative positions and widths of P and T waves to R peaks (for healthy subjects), as shown in Figure 15.

Reject noisy blocks: The blocks associated with small width are considered as blocks caused by noise. Blocks which are smaller than half of the expected size for P waves are rejected. Because the T waves are wider than the P waves, potential T waves are still present. The expected size for the P wave is based on the statistics for healthy adults, as described in [32] which varies from 90 ms to 130 ms. Blocks that are smaller than half of the width W_1 that is expected for the P wave are rejected.
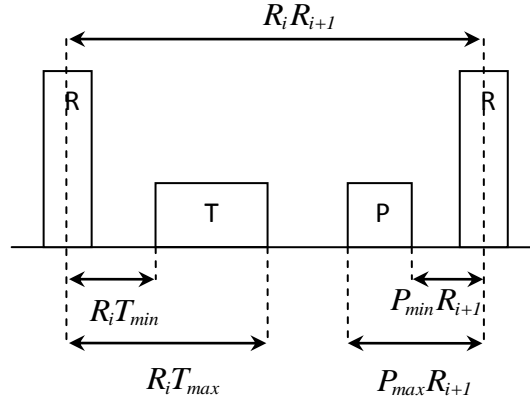
Figure 15 Demonstrating P and T wave time occurrence with respect to the current R peak and next the R peak. Where R_iT_{min} represents the minimum interval between the T wave and current the R peak, while R_iT_{max} represents the maximum interval between the T wave and the current the R peak. $P_{min}R_{i+1}$ represents the minimum interval between the P wave and next the R peak, and $P_{max}R_{i+1}$ represents the maximum interval the P wave and next the R peak.

In Arrhythmia ECG signals, P wave duration is smaller than in healthy adults. Therefore, the 75 per cent ratio has been set in order to consider these P waves that suffer from arrhythmia. This corresponds to:

$$P\_Block\ size = 0.75 * W_1 * (SF / 360) \qquad \text{Eq. 6}$$

where R_iR_{i+1} is the RR interval that contains the blocks of interest and *SF* is the sampling frequency. Similarly, T waves in arrhythmia ECG signals is smaller than in healthy people. Therefore, the block size of T wave will be double the P block size to detect small T wave durations as

$$T\_Block\ size = 1.25 * W_1 * (SF/360) \qquad \text{Eq. 7}$$

If *P_Block size* and *T_Block size* have been set equal to W_1 , the results will be close to the reported ones. Given the fact the P wave duration is smaller than T wave duration, support the idea of decreasing the expected P wave compared to the T wave.

Thresholding

To determine whether the detected blocks contain P or T waves, the number of blocks in each consecutive RR interval is counted. A threshold based on the distance of the maximum point within a block to the R peak is applied to distinguish P waves from T waves and noise.

There are three possibilities for the number of detected blocks:
1. Zero: the algorithm failed to detect a P or T wave in the current RR interval.
2. One: the P and T waves are most likely merged within one block, which is marked as an asterisk (see Figure 13 (b)).

3. More than one: The distance of the maximum point within a block to the nearest R peak will be used as a measure for selecting the blocks that contain potential P or T waves. This consists of two steps:
  a. *Detect potential T waves.* as shown in Figure 16, a block is considered to contain a T wave if the distance of the maximum point of the block to the nearest R peak is within a certain range.

$$R_iT_{min} = R_iR_{i+1}*0.111$$

$$R_iT_{max} = R_iR_{i+1}*0.583$$

YES — $max(BLOCK) > R_iT_{min}$ and $max(BLOCK) < R_iT_{max}$ — NO

T wave Block

Ignore Block
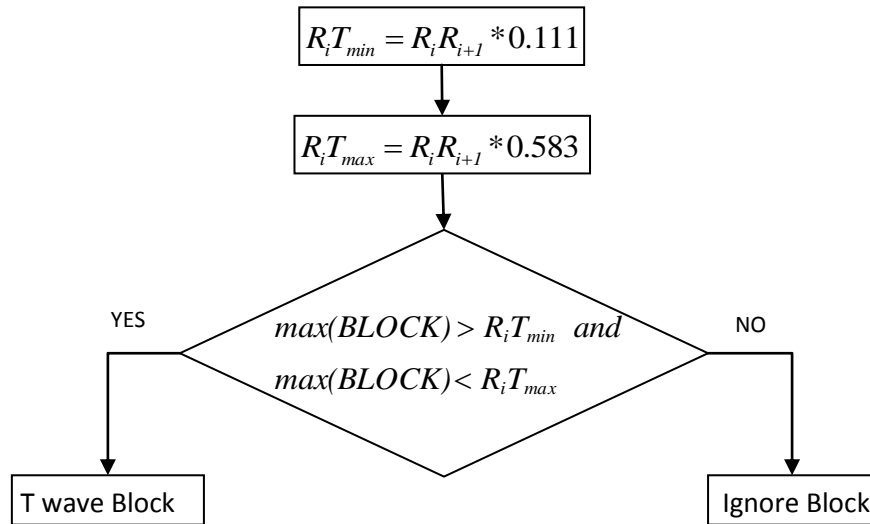
Figure 16 Flow chart for selection of T waves. If the block lies within the expected segment R_iT_{min} and R_iT_{max}, the block is considered to contain a T wave. The maximum absolute value within this block is considered as the peak of the T wave.

$$P_{min}R_{i+1} = 0.055*SF$$

$$P_{max}R_{i+1} = 0.47*SF$$

YES — $max(BLOCK) > P_{min}R_{i+1}$ — $max(BLOCK) < P_{max}R_{i+1}$ — NO

P wave Block

Ignore Block
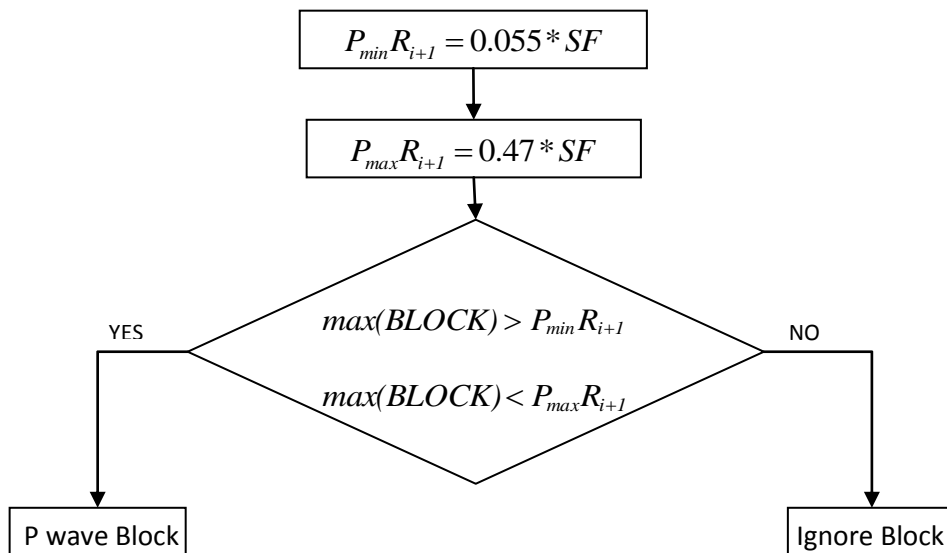
Figure 17 Flow chart for selection of P waves. If the block lies within the expected segment $P_{min}R_{i+1}$ and $P_{max}R_{i+1}$, the block is considered to contain a P wave. The maximum absolute value within this block is considered as the peak of the P wave.
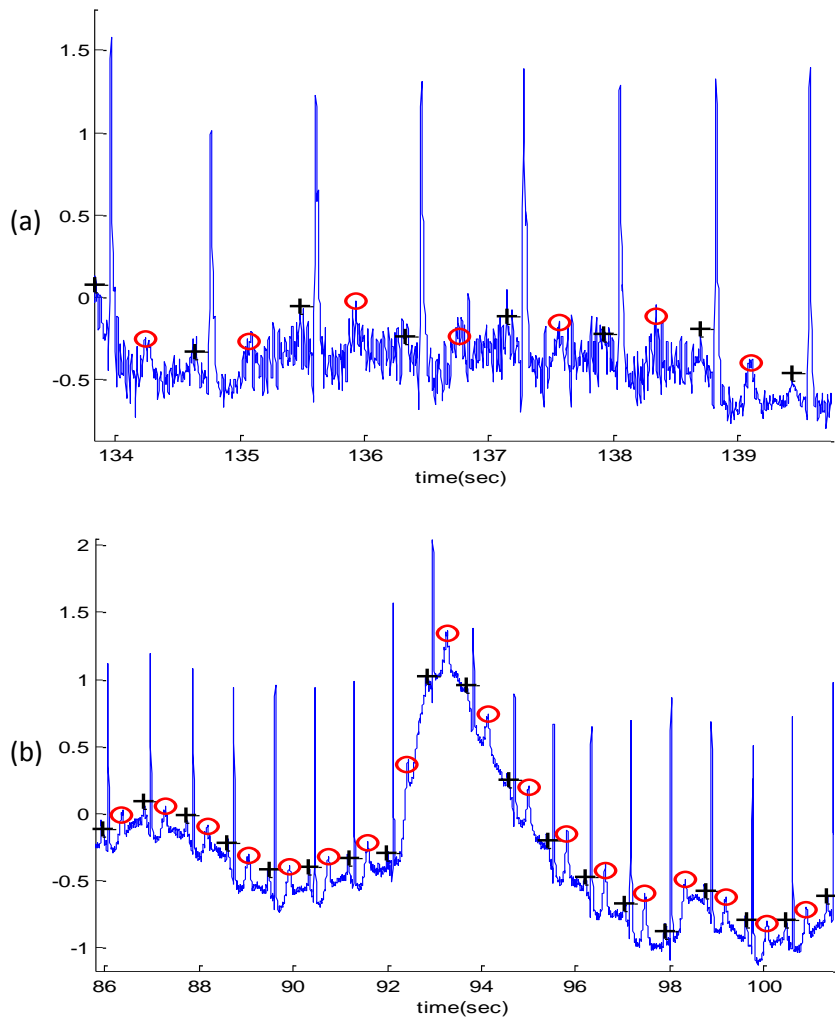
Figure 18 Demonstrating the performance of the proposed P and T detection algorithm. The algorithm succeeds to detect P and T waves in ECG signals that contain. (a) high-frequency noise, (b) baseline wander. '+' represents the P wave and 'O' represents the T wave.
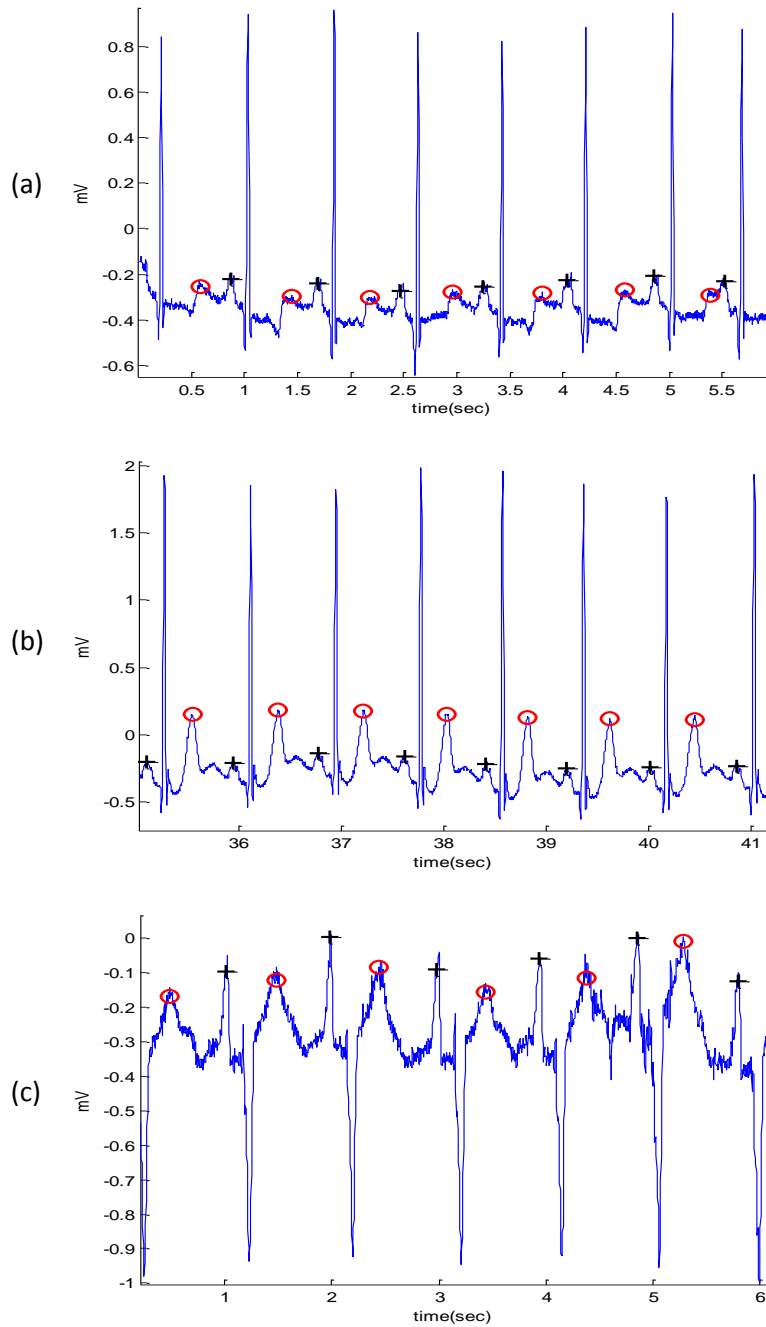
Figure 19 Demonstrating the performance of the proposed P and T detection algorithm. The algorithm succeeds in detecting P and T waves in ECG signals that contain (a) normal sinus rhythm without U waves, (b) normal sinus rhythm with U waves, (c) normal sinus rhythm with negative polarisation. '+' represents the P wave and 'O' represents the T wave.
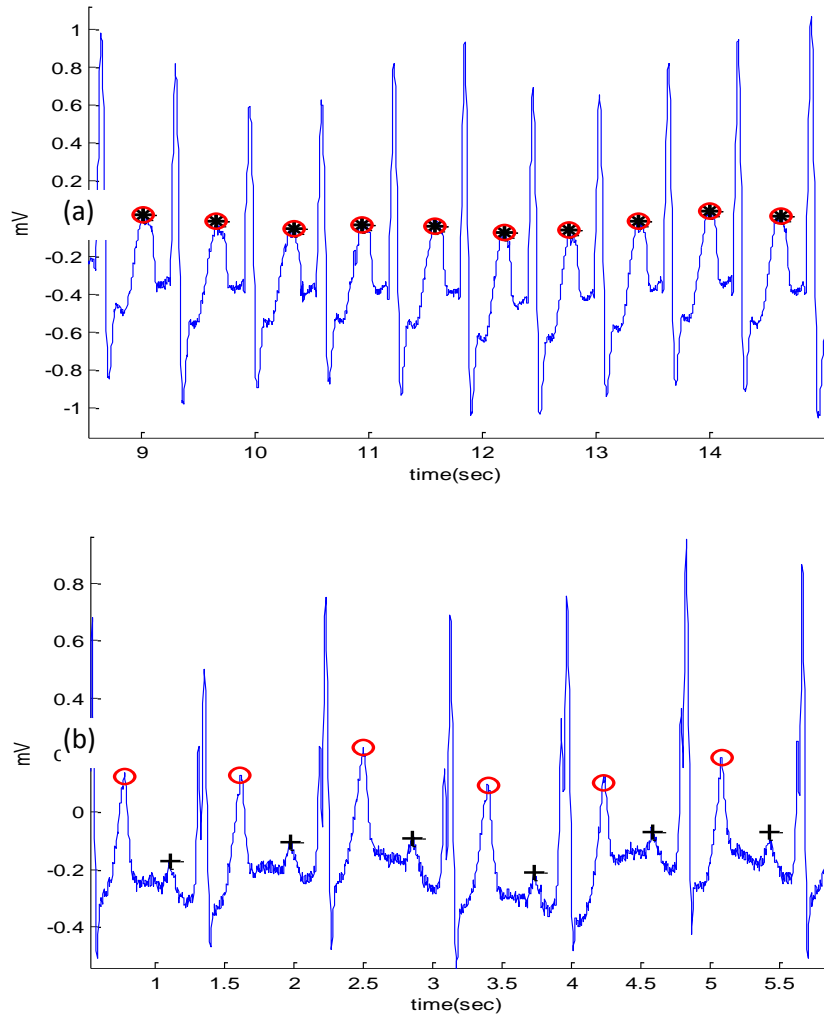
Figure 20 Demonstrating the performance of the proposed P and T detection algorithm. The algorithm succeeds in detecting P and T waves in ECG signals that contain a) LBBB beats with merged P and T waves, (b) LBBB beats. '+' represents the P wave and 'O' represents the T wave while the asterisk represents merged P and T waves.
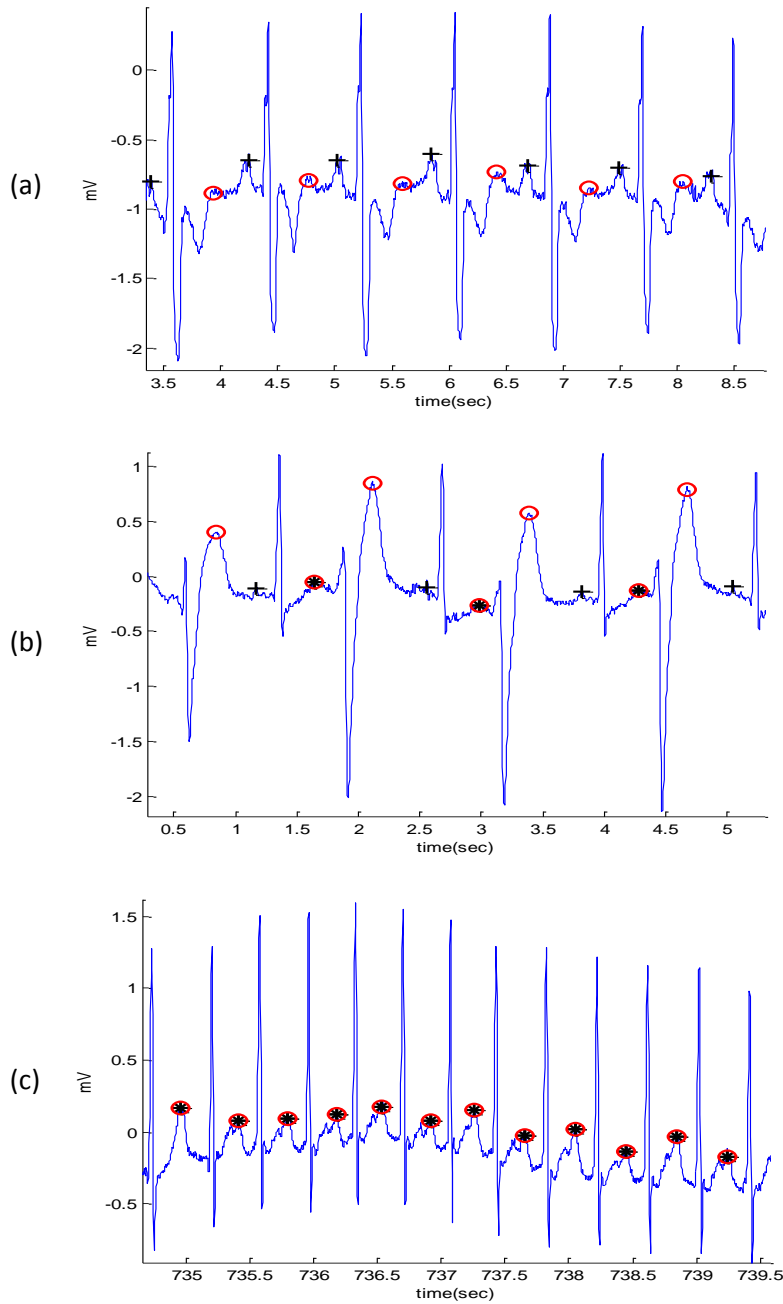
Figure 21 Demonstrating the performance of the proposed P and T detection algorithm. The algorithm succeeds in detecting P and T waves in ECG signals that contain (a) RBBB beat (record 118), (b) PVC beat (record 200), (c) PAC beat (record 209). '+' sign represents the P wave and 'O' represents the T wave, while the circle with asterisk represents merged P and T waves.

a. *Detect potential P waves*. As shown in Figure 17, consider a block as containing P wave if the distance of the maximum point of the block to the nearest R peak is within a certain range.

In some cases there is more than one block within the acceptable range for a P or a T wave. In these cases the block which contains the wave with the maximum amplitude is selected.

5. Results

The algorithm was evaluated using MIT−BIH database. The P and T waves were detected successfully even the merged P and T waves in arrhythmia ECG signals that are affected by: high-frequency, noise baseline wander, NSR, LBBB, RBBB, PVC, and PAC. All of the reasons for detection failure are described below.

1) ***High-frequency noise*.** high-frequency noise results from the instrumentation amplifiers, recording system and ambient electromagnetic signals received by the cables. The signal shown in Figure 18 (a) has been corrupted by power-line interference at 60 Hz and its harmonics and other high frequencies. As Figure 18 (a) illustrates, the proposed algorithm is very robust to noise.

2) ***Baseline wander*.** as shown in Figure 18 (b), the proposed algorithm is not sensitive to baseline wander and detected the P and T waves correctly.

3) ***NSR*.** is a normal ECG cycle is initiated by the sinoatrial node and consists of a P wave followed, after a brief pause, by a QRS complex, and then a T wave [5]. The proposed algorithms correctly detected P and T waves in three types of normal beats: 1) Normal sinus rhythm without U waves (record 100 of the MIT−BIH database) as shown in Figure 19 (a). 2) Normal sinus rhythm with U waves (record 103) as shown Figure 19 (b). 3) Normal sinus rhythm with negative polarization (record 108) as shown Figure 19 (c).

4) ***LBBB*.** results from conduction delays or blocks at any site in the intraventricular conduction system, including the main LBBB and the bundle of His. The result of an LBBB is extensive reorganisation of the activation pattern of the left ventricles [5]. The proposed algorithms successfully detected normal and merged P and T waves in two types of LBBBs: 1) LBBB beats with merged P and T waves (record 109), as shown in Figure 20 (a), and 2) LBBB beats with normal P and T waves (record 111), as shown in Figure 20 (b).

5) ***RBBB*.** is a result of conduction delay in a portion of the right-sided intraventricular conduction system. The delay can occur in the main RBBB itself, in the bundle of His, or in the distal right ventricular conduction system. RBBBs may be caused by a minor trauma such as right ventricular catheterisation [5]. As shown in Figure 21 (a), the proposed algorithms succeeded in detecting the P and T waves in ECG signals of RBBB (record 118).

6) ***PVCs*.** are characterised by the premature occurrence of a QRS complex that is abnormal in shape that has a longer duration than normal QRS complexes, generally exceeding 120 ms. The T wave is commonly large and opposite in direction to the major deflection of the QRS. The QRS complex is generally not preceded by a P wave, but it can be preceded by a non-conducted sinus P wave occurring at the expected time [5]. In Figure 21 (b), a special case of PVC is shown, called bigeminy, where the premature ventricular beats occur after every normal beat in an alternating pattern. The proposed algorithm succeeded in detecting the P and T waves in the normal beats and the T waves in the premature ventricular beats (record 200).

7) ***PACs*.** are among the most common causes of irregular pulses and can originate from any area in the heart [5]. The impulse is discharged prematurely by an irritable focus in the atria giving rise to a distorted P wave, usually superimposed on the preceding T wave. The P wave may be inverted. As shown in Figure 21 (c), the proposed algorithms detected the merged P and T waves in PACs (record 209).

Table 2 P wave detection performance over 10 records from the MIT−BIH Database

Record	No of beats	TP	FP	FN	SE	+P
100	2274	2274	0	0	100.00	100.00
101	1866	1866	0	0	100.00	100.00
102	2187	2021	87	79	96.37	96.02
103	2084	2076	4	4	99.81	99.81
104	2229	2071	82	76	96.58	96.32
105	2602	2557	33	12	99.53	98.72
106	2026	2013	12	1	99.95	99.41
107	2136	2136	0	0	100.00	100.00
108	1765	1363	244	158	90.56	86.13
109	2533	2342	135	56	97.72	94.67
	21702	**20719**	**597**	**386**	**98.05**	**97.11**

Table 3 T wave detection performance over 10 records from the MIT−BIH Database

Record	No of beats	TP	FP	FN	SE (per cent)	+P (per cent)
100	2274	2274	0	0	100.00	100.00
101	1866	1863	3	0	100.00	99.84
102	2187	2187	0	0	100.00	100.00
103	2084	2084	0	0	100.00	100.00
104	2229	2228	1	0	100.00	99.96
105	2602	2579	15	8	99.69	99.42
106	2026	2013	13	0	100.00	99.36
107	2136	2136	0	0	100.00	100.00
108	1765	1710	36	19	98.91	97.95
109	2533	2532	1	0	100.00	99.96
	21702	**21606**	**69**	**27**	**99.86**	**99.65**

As illustrated in Figures 18-21, the proposed method successfully detected P and T waves in ECG signals with a low SNR, baseline wander and various arrhythmias. However, the restults are reported in Tables 2 and 3 for just 10 annotated records of the MIT−BIH database, as discussed in section 2. The algorithm detects and evaluates the detected P and T waves automatically based on the following statistical parameters that are used to evaluate the algorithm:

$$Se_{P/T} = \frac{TP_{P/T}}{TP_{P/T} + FN_{P/T}} \qquad \text{Eq. 8}$$

$$+P_{P/T} = \frac{TP_{P/T}}{TP_{P/T} + FP_{P/T}} \qquad \text{Eq. 9}$$

True positive ($TP_{P/T}$): P/T wave has been classified as P/T wave.

False negative ($FN_{P/T}$): P/T wave has not been classified as P/T wave.
False positive ($FP_{P/T}$): non-P/T wave has been classified as P/T wave.

The sensitivity $Se_{P/T}$ is the percentage of true P/T waves that are correctly detected by the algorithm. The positive predictivity $+P_{P/T}$ is the percentage of detected P/T waves that are real P/T waves. Table 2 shows the result of P wave detection in 10 different records of the MIT−BIH database. P wave detection is affected by the quality of the ECG recordings and the abnormalities in the ECG signals. Records that have a relatively large proportion of very poor quality signals, such as 108 and 109, contain a larger number of FN than the other records. The arrhythmia P and T waves caused a large number of FP compared to the false negatives. False positives for P waves were often caused by a low signal to noise ratio. Ventricular premature beats and atrial arrhythmias occasionally caused false positives. The largest number of false positives was found in record 108. The sensitivity for P waves was 98.05 per cent and the positive predictivity was 97.11 per cent.

Table 3 shows the result of T wave detection in the same 10 records of the MIT−BIH database. The number of FNs was smaller than the number of FPs, as for P waves. FN were mainly caused by noise. FPs for T waves were often caused by PVC, as in record 108, and LBBB as in record 109. The algorithm achieved a sensitivity of 99.86 per cent and a positive predictivity of 99.65 per cent for T waves.

Table 4 P waves detection performance comparison. Several P wave algorithms have been compared on the MIT−BIH Arrhythmia Database (N/R: not reported).

Year	Algorithm	Method	Data used	Se (%)	+P (%)
2009	**Proposed algorithm**	**Blocks of Interest**	**10 records, 30 minutes each**	98.05	97.11
2009	Arafat et al. [34]	EMD	10000 normal ECG beats selected from the MIT−BIH database	N/R	N/R
2008	Diery [35]	WT	39 records, 10 seconds each, from the MIT−BIH database	N/R	N/R
2007	Mahmoodabadi et al. [36]	WT	Segments from the MIT−BIH database	51.69	53.64
2006	Ktata et al. [37]	WT	Segments from the MIT−BIH database	N/R	N/R
2005	Sun et al. [38]	Multiscale morphological derivative	Segments from the MIT−BIH database	N/R	N/R
2005	Goutas et al. [39]	Fractional order differentiation	Segments from MIT−BIH database that are suitable for just monophasic P and T waves	N/R	N/R
2004	Martínez [15]	WT	Applied to QTDB	N/R	N/R

Comparison of performance on MIT−BIH arrhythmia dataset

The detection performance on the MIT−BIH database obtained by the proposed P and T waves detector record by record performance (see Table 2, Table 3) and comparisons to other published detectors are provided in Tables 4 and 5. The P and T wave detection algorithm was evaluated using two statistical parameters: sensitivity

and positive predictivity. The data used to calculate these performance parameters are shown in the fourth columns of Tables 4 and 5. However, while the total number of records in the MIT−BIH aarhythmia Database is 48, most of the published P and T detection algorithms used few records or segments of the ECG signals, as shown in Tables 4 and 5. As shown, the algorithms published in the literature about detecting P and T waves in MIT−BIH database have limitations, which can be summarised as incomplete usage of the recorded ECG signals, detecting either P or T waves, and detecting particular morphologies of either P or T waves.

As shown in Table 4, the P wave detection algorithms in literature have been applied to few ECG segments. The proposed algorithm succeeds in handling long ECG recordings with high performance compared to the most recent and well-known publications in the P wave detection field.

A robust P and T wave detection algorithm is introduced against all challenges in Section 3. The algorithm succeeds in handling the non-stationary effects, low SNR, PACs, PVCs, LBBBs and RBBBs. The advantage of the proposed method is that it is numerically-efficient, robust, and it detects P and T waves simultaneously.

Table 5 T waves detection performance comparison. Several T wave algorithms have been compared on the MIT−BIH Arrhythmia Database (N/R: not reported).

Year	Algorithm	Method	Data used	Se (%)	+P (%)
2011	**Proposed algorithm**	**Blocks of Interest**	**10 records, 30 minutes each, from the MIT−BIH database**	99.86	99.65
2009	Arafat et al. [34]	EMD	10000 normal ECG beats selected from the MIT−BIH	N/R	N/R
2006	Ktata et al. [37]	WT	Segments from the MIT−BIH database	N/R	N/R
2006	Krimi et al. [40]	WT	Records from the MIT−BIH arrhythmia database	93	N/R
2005	Sun et al. [38]	multiscale morphological derivative	Segments from MIT−BIH database	N/R	N/R
2005	Goutas et al. [39]	Fractional order differentiation	Segments from the MIT−BIH database that are suitable for just monophasic P and T waves	N/R	N/R
2005	Sun et al. [38]	Multi-scale morphological derivative	False detections in biphasic T waves	N/R	N/R

As shown in Table 5, the T wave detection algorithms in literature have been applied to few ECG segments. The proposed algorithm succeeds in handling long ECG recordings with high performance compared to the most recent and well-known publications in the T wave detection field.

6. Discussion and conclusion

There is a limitation when evaluating P and T wave detection algorithms, as finding datasets with annotated P and T waves is quite difficult. Consequently,

comparing the existing algorithms becomes even more difficult. The devloped algorithm was evaluated using 10 records from the MIT−BIH database, containing a total of 21,702 heart beats annotated by two independed annotators, after runing the program, whether the P and T waves have been detected or not.

The algorithm successfully detected P and T waves in ECG signals with a low signal to noise ratio, baseline wander, and various arrhythmias. It achieved a sensitivity of 98.05 per cent and a positive predictivity of 97.11 per cent for P waves and a sensitivity of 99.86 per cent and a positive predictivity of 99.65 per cent for T waves. Moreover, the proposed algorithm succeeds to score the highest overall performance among the most recent and well-known publications in the P and T wave detection field.

It is clear from Tables 4 and 5 that the proposed algorithm is by far less complex compared to existing algorithms. The new algorithm has the advantage of being simple, fast and numerically-efficient. It is based on two moving average filters. The second moving-average window size equals the average P wave duration and the first moving-average window size equals half of the P wave. The second moving average works as a threshold to the first one. This creates blocks of interests followed by P and T wave duration thresholds to detect P and T waves

The assessment of the P and T detector has been reliably done over the existing standard databases. Moreover, the number of annotated beats used in testing the new algorithm is considered sufficient as it is a good representation of the possible morphologies found in ECG signals.

Unfortunately, the P and T waves in the MIT−BIH Arrhythmia Database are not yet fully annotated; this makes testing and evaluating developed algorithms quite difficult. However, a preliminary annotation for the used ECG signals will be uploaded to Physionet to allow validation by the clinicians and researchers. Moreover, further research should compare the performance of the proposed P and T detectors with more algorithms.

Acknowledgement

References

1. Australian Institute of Health and Welfare 2008 (2008) Australia's Health 2008. In: Australian Institute of Health and Welfare, editor. Canberra.
2. Australian Bureau of Statistics 2009 Causes of Death. In: Australian Bureau of Statistics 2009, editor. Canberra.
3. Global Cardiovascular Infobase. Ottawa, Canda: WHO Collaborating Centre on Surveillance of Cardiovascular Diseases, Surveillance and Risk Assessment Division, CCDPC, Public Health Agency of Canada and The Ottawa Hospital, University of Ottawa.
4. Australian Institute of Health and Welfare 2008 Australia's Health. In: Australian Institute of Health and Welfare, editor. Canberra.
5. Braunwald E, Zipes D, Libby P, Bonow R (2004) Braunwald's Heart Disease: A Textbook of Cardiovascular Medicine. Philadelphia: Saunders.
6. Trahanias P, Skordalakis E (1990) Syntactic pattern recognition of the ECG. IEEE Transactions on Pattern Analysis and Machine Intelligence 12: 648-657.
7. Willems JL (1988) Common Standard for Quantitative Electrocardiography Multilead Atlas − Measurements results Data Set 3 Commission of the European Communities − Medical and Public Health Research, Leuven.

8. Murthy ISN, Prasad GSSD (1992) Analysis of ECG from pole-zero models. Biomedical Engineering, IEEE Transactions on 39: 741-751.

9. Thakor N, Zhu Y (1991) Applications of adaptive filtering to ECG analysis: noise cancellation and arrhythmia detection. IEEE Transactions on Biomedical Engineering 38: 785-794.

10. Li C, Zheng C, Tai C (1995) Detection of ECG characteristic points using wavelet transforms. IEEE Transactions on Biomedical Engineering 42: 21-28.

11. Carlson J, Johansson R, Olsson SB (2001) Classification of electrocardiographic P-wave morphology. IEEE Transactions on Biomedical Engineering 48: 401-405.

12. de Azevedo Botter E, Nascimento CL, Jr., Yoneyama T (2001) A neural network with asymmetric basis functions for feature extraction of ECG P waves. IEEE Transactions on Neural Networks 12: 1252-1255.

13. Vila JA, Yi G, Presedo JMR, Fernandez-Delgado M, Barro S, et al. (2000) A new approach for TU complex characterization. IEEE Transactions on Biomedical Engineering 47: 764-772.

14. Strumillo P (2002) Nested median filtering for detecting T-wave offset in ECGs. Electronics Letters 38: 682-683.

15. Martinez JP, Almeida R, Olmos S, Rocha AP, Laguna P (2004) A wavelet-based ECG delineator: evaluation on standard databases. IEEE Transactions on Biomedical Engineering 51: 570-581.

16. Sovilj S, Jeras M, Magjarevic R (2004) Real time P-wave detector based on wavelet analysis. Proceedings of the 12th IEEE Mediterranean Electrotechnical Conference 1: 403-406 Vol.401.

17. Chouhan V, Mehta S (2008) Threshold-based Detection of P and T-wave in ECG using New Feature Signal. International Journal of Computer Science and Network Security 8.

18. PhysioBank Archive Index. Boston, USA: Physionet, Massachusetts Institute of Technology.

19. Moody GB, Mark RG. The MIT-BIH Arrhythmia Database on CD-ROM and software for use with it; 1990. pp. 185-188, open source available from:www.physionet.org.

20. Friesen GM, Jannett TC, Jadallah MA, Yates SL, Quint SR, et al. (1990) A comparison of the noise sensitivity of nine QRS detection algorithms. Biomedical Engineering, IEEE Transactions on 37: 85-98.

21. Rangayyan RM (2002) Biomedical Signal Analysis-A Case-Study Approach; Akay M, editor. New York, U.S.A,: John Wiley & Sons. 516 p.

22. Chang Yong R, Seung Hoon N, Seunghwan K. Conductive rubber electrode for wearable health monitoring; 2005. pp. 3479-3481.

23. Chen J (2010) Essentials of Technical Analysis for Financial Markets: Wiely.

24. Fong W, Yong L (2005) Chasing trends: recursive moving average trading rules and internet stocks. Journal of Empirical Finance 12: 43-76.

25. Gunasekarage A, Power D (2001) The profitability of moving average trading rules in South Asian stock markets. Emerging Markets Review 2.

26. Online Trading Concepts (2007).

27. Chen S, H.C. Chen, and H.L. Chan, (2006) A real-time QRS detection method based on moving-averaging incorporating with wavelet denoising. Computer Methods and Programs in Biomedicine 82: 187-195.

28. Thakor NV, Webster JG, Tompkins WJ (1983) Optimal QRS detector. *Medical and Biological Engineering* 21: 343-350.

29. Oppenheim A, Shafer R (1989) Discrete-time Signal Processing. NJ: Prentice Hall. 411-425 p.

30. Sahambi JS, Tandon SN, Bhatt RKP (1997) Using wavelet transforms for ECG characterization. An on-line digital signal processing system. Engineering in Medicine and Biology Magazine, IEEE 16: 77-83.

31. Elgendi M, Jonkman M, De Boer F. Premature atrial complexes detection using the Fisher Linear Discriminant; 2008. pp. 83-88.

32. Clifford GD, Azuaje F, McSharry P (2006) Advanced Methods And Tools for ECG Data Analysis. Artech House Publishers 1st edition.

33. Laguna P, Caminal P, Jane R, Rix H. Evaluation of HRV by PP and RR interval analysis using a new time delay estimate; 1990. pp. 63-66.

34. Arafat A, Hasan K. Automatic detection of ECG wave boundaries using empirical mode decomposition; 2009. pp. 461-464.

35. Diery A (2008) Novel Applications of the Wavelet Transform For Analysis of P Waves in Clinical ECG Recordings [PhD]. Australia: Griffith University.

36. Mahmoodabadi SZ, Alirezaie J, Babyn P. Bio-signal Characteristics Detection Utilizing Frequency Ordered Wavelet Packets; 2007. pp. 748-753.

37. Ktata S, Ouni K, Ellouze N. ECG Signal Maxima Detection Using Wavelet Transform; 2006 9-13 July 2006. pp. 700-703.

38. Sun Y, Chan KL, Krishnan SM (2005) Characteristic wave detection in ECG signal using morphological transform. BMC Cardiovascular Disorders 5.

39. Goutas A, Ferdi Y, Herbeuval J, Boudraa M, Boucheham B (2005) Digital fractional order differentiation-based algorithm for P and T-waves detection and delineation. ITBM-RBM 26: 127-132

40. Krimi S, Ouni K, Ellouze N. An Approach Combining Wavelet Transform and Hidden Markov Models for ECG Segmentation; 2008. pp. 1-6.